



Structure and Infrastructure Engineering

Maintenance, Management, Life-Cycle Design and Performance

ISSN: 1573-2479 (Print) 1744-8980 (Online) Journal homepage: <http://www.tandfonline.com/loi/nsie20>

Innovative technique for identification of prestressing tendons layout in post-tensioned bridges using a probe with MEMS accelerometer

Piotr Owerko & Marcin Honkisz

To cite this article: Piotr Owerko & Marcin Honkisz (2016): Innovative technique for identification of prestressing tendons layout in post-tensioned bridges using a probe with MEMS accelerometer, Structure and Infrastructure Engineering, DOI: [10.1080/15732479.2016.1212905](https://doi.org/10.1080/15732479.2016.1212905)

To link to this article: <http://dx.doi.org/10.1080/15732479.2016.1212905>



Published online: 25 Jul 2016.



Submit your article to this journal [↗](#)



Article views: 9



View related articles [↗](#)



View Crossmark data [↗](#)

Innovative technique for identification of prestressing tendons layout in post-tensioned bridges using a probe with MEMS accelerometer

Piotr Owerko^a  and Marcin Honkisz^b

^aFaculty of Materials, Civil and Environmental Engineering, University of Bielsko-Biala, Bielsko-Biala, Poland; ^bFaculty of Management and Transport, University of Bielsko-Biala, Bielsko-Biala, Poland

ABSTRACT

Post-tensioned concrete bridges are currently often constructed engineering structures. In this type of bridges it is crucial that geometrical layout of prestressing system complies with the design requirements. Unfortunately, major errors still occur during assembly of tendon routes. This has often negative effects. In a local aspect, it may cause a local damage, such as spalling of concrete cover. In a global aspect, prestressing may produce distribution of forces in the bridge structure different from the expected. That is why numerous methods have been developed to control the accuracy of executed tendon routs. Some of them, e.g. geodetic measurements with levelers, require direct access to tendon sheaths. Other methods, which can be used after casting of concrete (mainly NDT methods) have a series of resolution, efficiency and accessibility limitations. Hence, the paper presents a proposal of an alternative method for control of tendons routing using a special probe with Micro Electro-Mechanical Systems capacitive accelerometer. The paper presents a concept of tests performed with the probe, evaluation of the probe application in the view of a random process and finally assessment of the results obtained with the use of the constructed measurement system in trial laboratory conditions.

ARTICLE HISTORY

Received 29 March 2016
Revised 12 May 2016
Accepted 27 May 2016

KEYWORDS

Post tensioning; bridges; concrete; cables & tendons; non-destructive testing; random processes; assessment; measurement

Introduction

Post-tensioned concrete bridges are currently one of the most commonly executed engineering structures. Prestressing tendons placed in these structures on dedicated routes on one hand allow to achieve greater slenderness of the elements, impossible for traditional reinforced concrete girders, and on the other to use modern technologies of construction accelerating the investment process. For a structure to behave as theoretically assumed, it is crucial that geometrical layout of the prestressing system complies with the design requirements. Nevertheless, as it can be concluded from the literature of the subject, major errors still occur during assembly of tendons, which are misplaced in an uncontrolled way during casting of concrete, and which result in considerable differences between the designed and executed tendon routes.

The knowledge of good approximation of the real tendon route is very important to evaluate if the structure behaves properly. It is especially important in continuous systems, in which the effect of prestress can induce additional reactions and moments, and the analysis of these influences requires relatively accurate representation of tendon's route in a computational model. The knowledge of the prestressing system layout can be therefore essential in future expert calculations or in planning of strengthening works. Very often it facilitates detailing of the range and type of repair works in older post-tensioned structures.

Therefore, the authors started this paper with synthetic presentation of the examples of bridges in which major mistakes were made during assembly and concreting of tendon sheaths. Negative effects of these errors were also discussed. Finally, a brief overview was made of the methods for control of tendon routing as well as of identification and efficiency limitations of geodetic and NDT methods.

The most important paragraphs are related to the proposal of an alternative method for investigation of tendon route layout in newly constructed structures. This method incorporates a Micro Electro-Mechanical Systems (MEMS) capacitive accelerometer embedded in a custom-designed probe moving inside an empty tendon sheath (cable canal).

Examples of errors during assembly and concreting of tendon sheaths

Negative effects of errors during assembly of prestressing tendon sheaths are well known since the beginning of a widespread use of post-tensioned concrete. In the description of one of the most famous examples in Central Europe (Biliszczyk, 2013; Flaga & Kisała, 2013; Łaziński & Salamak, 2015) it has already been pointed out that in 1984 French Ministry of Transportation published an appropriate instruction related to this issue. Nevertheless, such problems still reoccur in post-tensioned concrete bridges, regardless of the type and size of the structure.

They appear in structures of different types: slab, beam, box and even modern *extradosed* structures.

The first of the presented examples are two groups of not yet concreted sheaths in a certain bridge structure (Figure 1). Cable group in the third background was assembled properly and its layout was close to the designed route. Sheaths were attached to the bottom rebar with the use of special frame-shaped supports. During the assembly of three sheaths, visible in the foreground, a gross error was made: elements were placed on a top bar of the frames. This caused serious deviation from the project. Trajectory of the sheaths was changed on a significant area, including anchorage zone. In consequence, there was an increased probability that the behaviour of the structure would be considerably different than assumed during calculation of the prestressing effect (Aalami, 2000; Choi, Kim, & Hong, 2002).

Sheaths can be also misplaced during casting of concrete mix. The possibility of such a problem in real structures is emphasised by leading prestressing system producers in their technical approvals (BBR, 2013; Dywidag, 2013; Freyssinet, 2010). It has also been confirmed by the work (U.S. Federal Highway Administration, 2013). Similar mistake was made in a railway concrete slab bridge (Figure 2). During assembly of sheaths and concreting several serious imperfections arose. This resulted in local spalling of concrete cover around one of the side tendons on the area of around one square metre (Figure 2). Thick, 20 mm stirrups were bent and cable sheaths became visible on the outer surface. The cause was a major imperfection in tendon assembly, both in plane and in vertical position. During visual inspection it was observed that deviation of cable layout in vertical direction was as much as 25 cm. Consequently, the curvature of the route was in this location opposite to the required.

Another object in which damage was caused by errors in assembly of tendon sheaths was an extradosed-type bridge MA 532 along the A1 highway in Mszana, southern Poland (Figure 3). This problem, famed in local media, was related mainly to the bottom slab of one of the span segments. During prestressing of tendons, concrete cover spalled at the length of 3.0 m and width of 2.0 m (Biliszcuk, 2013; Flaga & Kisała, 2013). The magnitudes of the errors were considerable. Undesirable differences of relative vertical coordinates of the assembled sheaths with respect to the values assumed by the designer were equal to 10 and 7 cm at the length of 2.8 m (Figure 4). At the distance of 1.4 m, wrongly executed routes of two cables could have been approximated with polynomial curves with sags (at this distance) of 4.9 and 3.4 cm. Assuming such simplification, undesirable vertical forces acting on the concrete cover were determined. They were equal to 964 and 668 kN, respectively.

Certainly, the discussed problems are not limited to Central Europe. Similar examples were reported in (Ruan, Shi, & Li, 2012), (Landuyt, 1991), (Podolny, 1985). Cruz, Topczewski, Fernandes, Trela, and Lourenço (2010) showed that the problem of erroneous assembly of tendon sheath had consequences during repair and strengthening of a structure. After preliminary destructive tests it appeared that mistakes in the prestressing system were so serious that they collided with the chosen strengthening system. Therefore, georadar inspection of the actual location of tendons was performed in order to safely assemble strengthening elements (steel deviators).

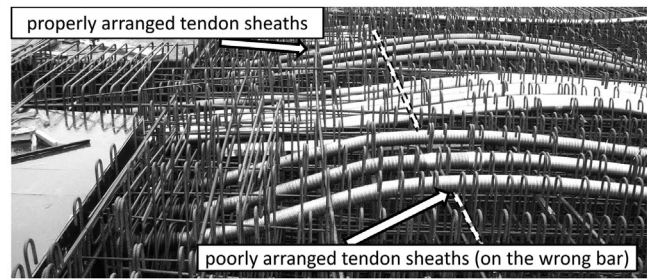


Figure 1. Error in assembly of tendon sheaths – related to the whole cable group.

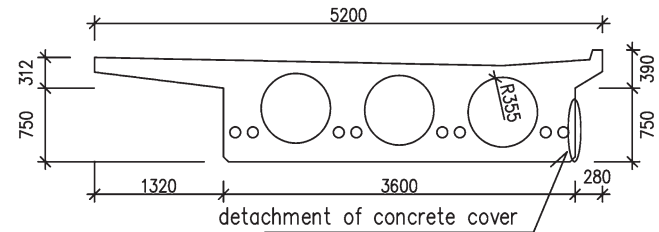


Figure 2. Location of concrete cover spalling in a cross section.



Figure 3. MA-532 Extradosed bridge during strengthening.

The discussed errors in tendon sheaths' routes have also consequences in the durability of the executed structures. Local imperfections can lead to reduction of the required concrete cover thickness (EN 13670, 2009). This may, in turn, lead to direct risk of corrosion of the prestressing system element (U.S. Federal Highway Administration, 2013). The second problem can arise from difficulties in cement injection process, especially in the zones of local unexpected changes of its route. It may be accompanied with the risk of entrapment of air near the high point of tendon route. According to Martin, Broughton, Giannopolous, Hardy, and Forde (2001) this may cause unsatisfactory anti-corrosive protection of tendons as well as improper cooperation between tendons and adjoining concrete.

Methods for control of correctness of tendon sheaths layout

It has been shown that the consequences of the discussed errors can be very serious. That is why control of prestressing tendon sheaths' layout is one of the routine actions recommended by the supervision inspector on the building sites of post-tensioned

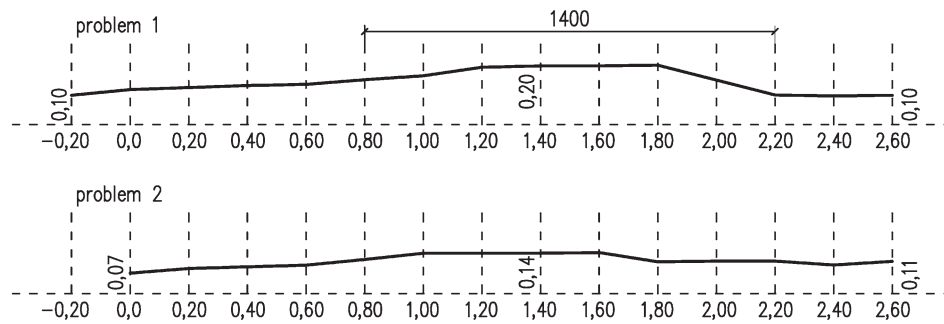


Figure 4. MA-532 measured routes of chosen tendons in longitudinal section (based on: Flaga & Kisala, 2013).

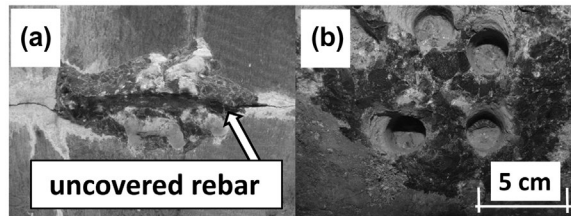


Figure 5. (a) Example of uncovering of concrete cover. (b) Example of drilling.

concrete bridges. Most often it is a traditional geodetic measurement with the use of levels or tachymeters (Gocał et al., 2013).

Decision to allow concreting depends on the results of comparison between the measured coordinates of the sheaths and the designed route, accounting for the tolerances agreed in the contract, often according to the recommendations (EN 13670, 2009). These methods require, however, direct access to the sheaths. Therefore, measurements have to be made before casting of concrete. It has also been mentioned that uncontrolled movement of the pipes can occur during casting of concrete mix. Hence, inventory of sheaths before concreting is not always sufficient to confirm compliance of the sheath routes with the design project.

For many years destructive (invasive) techniques were dominantly used to localise sheaths after casting of concrete. Exemplary effects of drilling and uncovering of concrete cover are shown in Figure 5. They are often very labour-demanding and pose a risk of damage to the elements of prestressing system, which has been confirmed in i. a. (Cruz et al. (2010)). In general, since the beginning of twenty-first century spectacular development of NDTs has been observed. The overview of these methods in the context of concrete structures' testing has been presented by International Atomic Energy Agency (2002) and Verma et al. (2013). Table 1 collectively presents these techniques which are the most important for localisation of prestressing tendons.

As it has been shown in e.g. (Topczewski, 2007), radiography can be very efficient in recognition of the prestressing elements. The work (Dérobert, Aubagnac, & Abraham, 2002) points out, however, its drawbacks. According to the presented observations, good access to the X-rayed element from both sides is required and the dimensions of the element cannot be too small. Limitations have been also emphasised connected with necessary radiological protection of the operator and neighbouring natural environment. Therefore, intensive development of alternative methods has been observed recently, including radio- and micro-wave techniques as well as acoustic techniques.

For inspection of the location of tendons, profometers appear to be also useful tools (Silvestri & Williams, 2012). Measurements are performed with the use of special measuring coils accounting for the phenomenon of eddy currents formation in the neighbouring ferromagnets. As it has been shown in (Dérobert et al., 2002), applicability of the device for detection of tendons is limited only to small depths, and in case of dense and thick reinforcement, which is usually present in bridges, the device is inefficient.

Georadar method is one of the radio-wave (or micro-wave) methods which uses the changes undergone by the electromagnetic wave emitted inside the medium. Its theoretical basis has been described in e.g. a monograph (Daniels, 2004). Finally, the acoustic methods – impact echo (IE), Ultrasonic echo (UE), Ultrasonic shear wave test method (USW) – are based on the emission of, respectively, acoustic impulses, ultrasonic waves and multitransducer emission of mechanical transverse waves (De La Haza, Samokrutov, & Samokrutov, 2013).

The listed NDT methods (especially Ground penetrating radar (GPR)) have been recently used for inspection of the location of tendon sheaths and reinforcement. Their efficiency in inspection of the prestressing tendons in in-situ measurements of real engineering structures has been analysed in e.g. (Cruz et al. (2010); De La Haza et al., 2013; Dérobert et al., 2002; Kohl & Streicher, 2006). In georadar and acoustic laboratory tests, except for the sole localisation of sheaths, the quality of tendon grouting is also analysed. The use of GPR techniques for this purpose has been described in e.g. (Cheilakou, Theodorakeas, Kouli, Moustakidis, & Zeris, 2013; Kohl & Streicher, 2006; Muldoon, Chalker, Forde, Ohtsu, & Kunisue, 2007; Zhou, Luan, & Zhang, 2013), while the use of acoustic techniques has been presented in (Ata, Mihara, & Ohtsu, 2007; Martin et al., 2001). This problem is also reflected in modern technological solutions of prestressing systems, such as prefabricated injection and the use of transparent sheaths for external prestressing, described by Mutsuyoshi, Hai, and Kasuga (2008). An important branch of georadar tests is also detection of other anomalies in the internal structure of a concrete element such as voids and discontinuities (Xie, Qin, Yu, & Liu, 2013; Yehia, Qaddoumi, Farrag, & Hamzeh, 2014).

In a majority of the referred tests (especially those using GPR) satisfactory results of tendons' inspection were reported. In case of a viaduct described by Cruz et al. (2010) this allowed to even change and detail a repair programme. It must be, however, noted that a lot of the referred publications of the discussed tests are related to the elements characterised by simple geometry and with moderate intensity of reinforcement. In the publications disadvantages and limitations of the georadar and acoustic

Table 1. NDT methods used for localisation of prestressing tendons.

Technique	Abbreviations	Principle of operation	Selected practical remarks
Radiography	X-ray γ-ray	Emission and absorption of X-rays or γ-rays	+ High identification efficiency and resolution power – Measures for radiological protection required – Access from both sides to the element required
Covermeter	–	Electromagnetic induction, tracking changes in voltage	+ Relatively low device costs + Does not require handling by expert – Very limited identification depth – Only detects ferromagnetics
Ground penetrating radar	GPR	Electromagnetic emission (microwaves or radiowaves)	+ Well tested and often used in field research + Effective in detection of tendons and voids – Dense reinforcement can be a major hindrance – Experience required for the interpretation of data
Impact echo	IE	Controlled emission of acoustic pulses	+ Potential for determining the quality of grouting – Dense reinforcement can be a major hindrance – Can be very time-consuming in the practical use on large surface areas
Ultrasonic echo	UE	Emission of ultrasonic waves	+ Relatively low cost of the device – Dense reinforcement can be a major hindrance – Coupling agent required – Can be very time-consuming in the practical use on large surface areas
Ultrasonic shear wave test method	USW	Multi-transducer emission of transverse, ultrasonic waves	+ One of the most modern and advanced techniques + No coupling agent required + Automated process of data interpretation – Still insufficiently tested in various field conditions – As all the above techniques often requires a telescopic boom lift or scaffolding usage – Relatively high device costs

techniques were revealed. A fundamental limitation of many emission techniques is a fact that as a consequence of an increase of the resolution of the equipment (using higher frequencies of signals) a possible penetration depth is decreased.

Some remarks are also related to more practical limitations. Cruz et al. (2010) and Topczewski (2012) point out difficulties in realisation of GPR tests on rough, uneven surfaces. Topczewski (2012) says also that the tests cannot be performed on humid elements (also on early age concrete). An important aspect is high labour demand of the discussed NDTs and accessibility to specific areas of a structure. A telescopic boom lift or scaffolding has to be often used to perform NDT scanning on spans elevated high above the ground level, which is an arduous and labour-demanding process. The discussed problems were also observed by the first author during execution of the tests on the elements with high intensity of reinforcement covering the searched sheaths (Owerko & Ortyl, 2013; Owerko, Ortyl, & Salamak, 2013).

Proposal of a probing method with MEMS-type accelerometer

In view of the collected conclusions, the authors decided to commence works on an alternative measurement method independent of the before-mentioned limitations. The main goal of the research described in this section was an attempt to develop a method for control of newly executed structures in which the post-tensioned tendon routes are tracked with the use of a custom-made measuring probe with a built-in MEMS capacitive accelerometer.

MEMS accelerometers have found numerous applications in the concrete construction industry (Kavitha, Joseph Daniel,

& Sumangala, 2016). They are embedded in e.g. inclinometers which are used for control of potential landslides, as shown in (Geokon Incorporated, 2015). In this paper a similar inclinometer is presented (although it does not apply a MEMS accelerometer), dedicated to inspect horizontal displacements. It allows to control the behaviour of linear objects, e.g. uneven settlements of important railway sections or large hydrotechnical structures. Recently, MEMS accelerometers have been used for monitoring of bridge structures. Chae, Yoo, Kim, and Cho (2012) presented that they were used for indirect measurement of tension in hangers of *Yongjong* arch bridge in South Korea.

Idea of the method

The technique proposed by the authors involves multiple passages of the probe with accelerometer inside a sheath (cable canal) with registration and interpretation of data (Figure 6). This measurement method is potentially independent of such conditions as:

- Elevation of a structure above the terrain level (accessibility requirements),
- Density of reinforcement covering searched tendon sheaths,
- Geometry of the cross section of the tested object.

The inclination angle of the probe with respect to the horizontal position in the vertical plane parallel to the axis of the probe as well as the length of the past passage (the length of the pulled rope at the moment of measurement) are measured in equal time intervals (100 ms). The measured values of inclinations

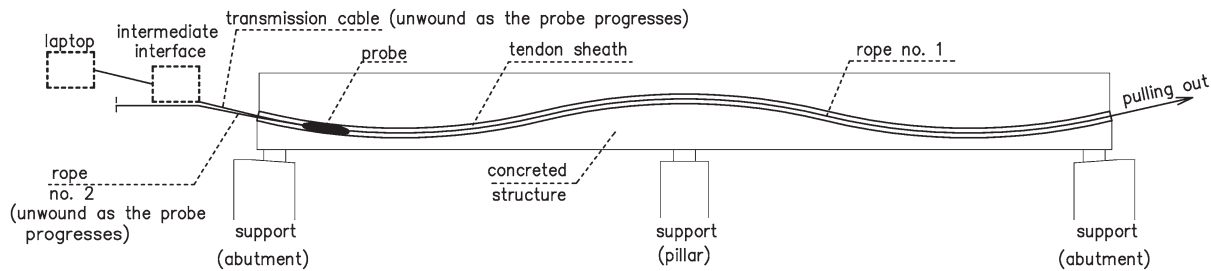


Figure 6. Idea of sheaths' route measurement with the use of the probe.

are registered with the intermediary interface and laptop as corresponding changes of direct current voltage occurring in three-dimensional accelerometer. Then, a function is used which describes the relationship between the voltage and the inclination angle of the probe. After such conversion, a signal is treated with a special algorithm allowing to re-calculate the registered data into vertical and horizontal location of the probe in respective points of the route.

Potential range of application

The described measurement technique was developed for geometrical inspection of tendon sheaths in post-tensioned concrete bridges. Nevertheless, if properly modified, it could be also used in general building industry, e.g. in post-tensioned concrete floor girders. At the same time, fundamental limitations of the method should be noted, i.e. necessity to perform the tests before installation of prestressing strands (Figure 6). The method is also limited to newly executed structures in which the strands are installed after concrete casting. Therefore, some segmental structures cannot be tested with the use of this method if they were designed with joint heads or passive anchorage (Freyssinet, 2010). These elements require hauling of strands before casting of concrete mix. They are popular in incrementally launched bridges or bridges executed in the span-by-span technology (Zilch, Weiher, & Riesemann, 2007). Described technique cannot be also used in the objects with prefabricated cables.

It must be noted, however, that the number of structures in which the strands are installed after casting of concrete is large and it can be thought that these types of structures will be popular in future. This group of structures includes, e.g., typical beam highway bridges, presented by e.g. Łaziński and Salamak (2011), as well as a part of structures equipped with anchoring protrusions (continuity anchor blisters). These concrete components are more and more often used in bridges with a static scheme of a continuous beam. They allow for elimination or reduction of the joint heads number.

It must be emphasised that the proposed technique allows only to effectively determine the tendons' route. Accelerometer has no capability to detect voids or evaluate thickness of the concrete cover. The latter can only be assessed indirectly by comparison of the collected images of the routes with the inventory documentation of the girder. Hence, the aim of the presented approach was not to criticise or diminish the existing NDT techniques but

solely to present possibilities provided by an alternative method for efficient control of the accuracy of tendon sheaths' assembly. Elements of the prototype measurement system.

The developed measurement system (Figure 7) is composed of the following elements:

- Openable casing with a bottom (2) and top part (3),
- Three-dimensional accelerometer (1),
- Voltage stabiliser (6),
- Connecting wire (5) with external system registering measurement data,
- Intermediary interface (4),
- Laptop registering data.

The built probe is a prototype version. It was created as an effect of long and arduous tests. The casing must have to fulfil the following requirements during the testing passages:

- Efficient protection of the integrated circuit,
- Constant inclination angle of the integrated circuit with respect to the bottom of the sheath (especially in vertical plane parallel to the axis of the route),
- Smoothness of passage along the notches of the sheath and easiness to stop the probe in the location chosen by the operator,
- Short distance in plane between the axis of the casing and the axis of the sheath at the whole length of the route,
- Resistance to atmospheric conditions, humidity, contamination, impact, etc.
- Ease of passage along curvilinear segments of the route, even at the arcs with small radii (the minimum radii of the arcs were assumed based on the technical approval (BBR, 2013).

After numerous tests on different types of casings it appeared that the best performance can be obtained with a casing of a shape of an oval capsule made of solid timber built in the technology of timber turning. In the authors' opinion the diameter of such probe should be around 80–85% of the internal diameter of the tendon sheath. This will prevent chocking of the probe at arc segments. In order to limit vibrations of the probe it is recommended that the length of the casing is at least five times its diameter. The nest for the integrated circuit should be located in the centre of gravity of the casing. A relatively heavy ballasting element should be placed below to lower the centre of gravity of the probe.

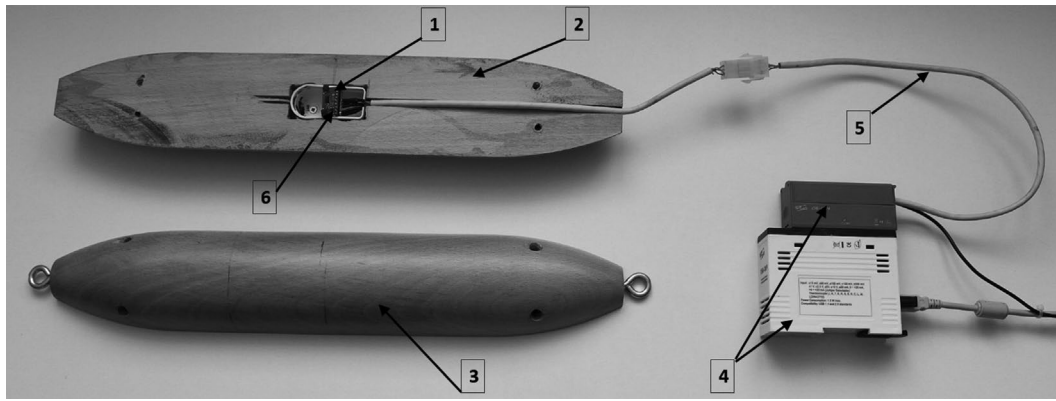


Figure 7. Elements of measurement system.



Figure 8. Testing route after construction in the laboratory.

Testing of the probe

Laboratory testing route

Testing route with the length of 6.0 m was made of two segments of BBR[®] corrugated pipes ($\varnothing_{\text{int}} = 95 \text{ mm}$), properly merged, bent and placed on previously prepared wooden supports (Figure 8). It is composed of two arcs with an internal radius of 6200 mm (Figure 9). The design of the route assumed equal coordinates of the beginning and end of the route. A difference between the highest and the lowest point of the route's axis was assumed to be equal to 358 mm. The route was constructed thoroughly to reflect the designed route as precisely as possible. Inventory of the route was made with a precise leveler *Zeiss Koni Ni007*[®]. The results obtained in 21 control points were considered in further analyses as reference points.

Method of passing of the probe inside the canal

After long-term tests on the testing route, it was finally decided that interval pulling of the probe inside the sheath would be applied. Pulling of the probe was therefore realised with stops

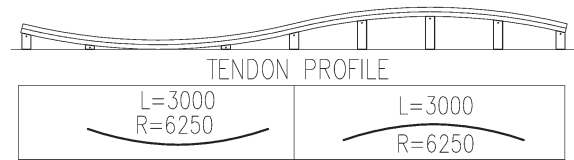


Figure 9. Geometry of testing route.

at equal distances of the passed route. The ropes for pulling were marked at every 30 cm. This follows the recommendations for testing tendons' layout in bridges given by Topczewski (2012). The probe was moving at the speed in the range of .1–.2 m/s along the distance of 30 cm, and then it was each time stopped. The total time of a single interval (30 cm passage and stop) lasted about 10 seconds. Voltages, and therefore inclinations of the probe, were read in equal intervals every 100 ms. Readings were made both during movement and during stops. Undoubtedly, interval pulling is more time-consuming than pulling with constant speed. Single passage through the canal of 6 m length lasted about 200 seconds, which gives about .5 mins for testing of 1 m of a route. This method has two principal advantages, though. The first one is simplicity of implementation in testing. There is no need for electric breaching nor skilled probe's operator. The second one is no influence of undesirable accelerations' resultants on the registered measurements of the accelerometer. During stops, vibrations attenuate and centripetal force decays. During each stop, more stable voltage image is obtained which provides more relevant measurements of the probe's inclinations (Figure 10).

Repetitive tests – experiment in the view of random process

Nine passages were taken into consideration for analysis, designated as p_1, p_2, \dots, p_9 . They were realised on a testing route in the interval mode. All the passages were performed on the same day, one after another, without switching off the measuring equipment. Each interval in a given trial, which means a passage along the length between the subsequent markers with a stop, lasted around 10 s. All the test passages were conducted in the same direction. Each time the probe with a casing (Figure 7) was placed in such a way that its centre coincided with the starting

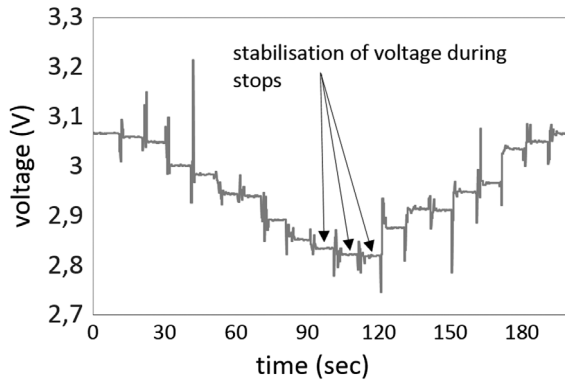


Figure 10. Stabilisation of voltages from accelerometer at stopping of the probe in canal.

point of the route. The distance between the stops was equal to 30 cm, which corresponded to the distance between the markers on the rope.

The described tests had two main aims. The first aim was to evaluate repeatability of the registered voltages from accelerometers in relation to subsequent passages and intervals. The second, not less important aim, was to find a universal time interval in which there was a very high probability that the probe stopped and the registered voltages were stabilised. Such an analysis allowed to build an algorithm for tracking of a travelled route. For that purpose, in all intervals of subsequent realisations the analysis was made of the images and values of voltages in time as well as the estimators:

- Standard deviations of voltage,
- Autocorrelation function,
- Autocovariance function.

Standard deviation of a random function $X(t)$ was expressed with a well-known relationship (Papoulis & Pillai, 2002), where E is an operation of finding the expected value:

$$\sigma(t) = \sqrt{E\{[X(t) - E(X(t))]^2\}} \quad (1)$$

Having a finite number of realisations of the process ($m = 9$ realisations) the following estimator of standard deviation was accepted as satisfactory:

$$\tilde{\sigma}(t) = \sqrt{\frac{\sum_{i=1}^m \{[x_i(t) - \tilde{x}(t)]^2\}}{m - 1}} \quad (2)$$

The expected value of the random function $\tilde{x}(t)$:

$$\tilde{x}(t) = E[X(t)] \quad (3)$$

The expected value of the random function at time t was estimated with the mean value of realisation:

$$\tilde{x}(t) = \frac{1}{m} \sum_{i=1}^m x_i(t) \quad (4)$$

The autocorrelation function $\Gamma_x(t_1, t_2)$ of the random function $X(t)$ was given by the expression:

$$\Gamma_x(t_1, t_2) = E\{[X(t_1)][X(t_2)]\} \quad (5)$$

The following estimation of the autocorrelation function was taken:

$$\tilde{\Gamma}_x(t_1, t_2) = \frac{1}{m} \sum_{i=1}^m \{[x_i(t_1)][x_i(t_2)]\} \quad (6)$$

A variable τ was also introduced according to the relationship:

$$\tau = t_2 - t_1 \quad (7)$$

The autocovariance $K_x(t_1, t_2)$ of the random function $X(t)$ was given by the expression:

$$K_x(t_1, t_2) = E\{[X(t_1) - \bar{x}(t_1)][X(t_2) - \bar{x}(t_2)]\} \quad (8)$$

The following estimation was assumed:

$$\tilde{K}_x(t_1, t_2) = \frac{1}{m} \sum_{i=1}^m \{[x_i(t_1) - \tilde{x}(t_1)][x_i(t_2) - \tilde{x}(t_2)]\} \quad (9)$$

After the analyses it appeared that the estimators of the expected value (Figure 11), standard deviations, values of the autocorrelation function and the autocovariance function stabilise (have similar, relative values) in the areas corresponding to the stop of the probe in a given interval. It was also noted that a significant drop in standard deviation was observed there, and the value of the autocovariance function was close to zero. Constant values of the autocorrelation function, autocovariance function and mean of the signals are characteristics of the stationary process (Papoulis & Pillai, 2002). Therefore, if the periods of stops of the probe in subsequent intervals were treated as separate random processes then they could be classified as stationary. Moreover, it was observed that the values of standard deviations and autocovariance function during stops did not increase with the succeeding intervals. It could be then concluded that the distribution of the registered voltage values did not increase with an increase in length from the beginning of the route.

The obtained results could have been further analysed in detail, i.e. in relation to the individual intervals. First of all, it allowed to show better that the registered process in some areas has features of a stationary process. Secondly, it was easier to determine the time interval in which the probe stops and voltages (inclinations of the probe) are stabilised. Figures 12(a) and (b) relate to the voltage image and autocovariance function, respectively, $\tau = 10$ s in an interval no. 9. Presentation of the results was therefore limited to one exemplary interval. The results for the remaining intervals were analogous.

Based on the analysis of all intervals it was observed that the signal stabilises between the 5th and 9th second of a given interval in each of the passages. This time interval was marked in appropriate diagrams (Figure 12). To calculate the coordinates of the passed route, a median of 40 readings of voltage in a given interval could be used. In the finally applied algorithm, shown in Figure 13, a mean value of the narrower period was used: 10 readings of the 8th second in each interval were considered. Additional analyses with the use of appropriately adjusted statistical tests showed that such a limited range was proper for further calculations.

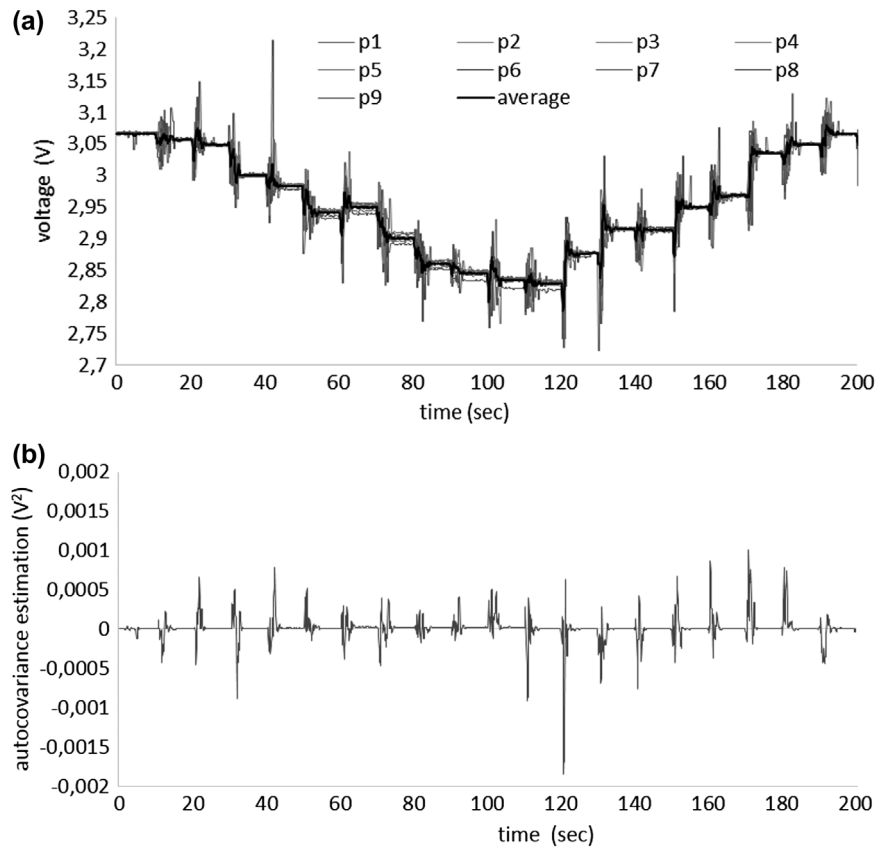


Figure 11. Estimation of the expected value of voltages and autocovariance function – whole process. (a) voltage – all 9 runs. (b) autocovariance – $\tau= 10$ [s].

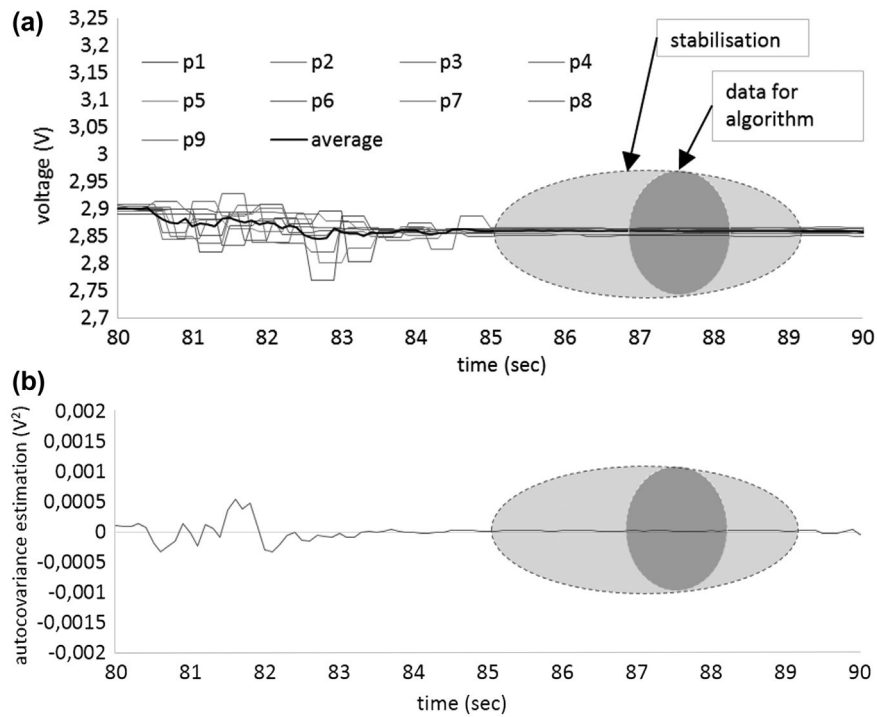


Figure 12. Estimation of the expected value of voltages and autocovariance function – chosen interval no. 9. (a) voltage – all 9 runs. (b) autocovariance – $\tau= 10$ [s].

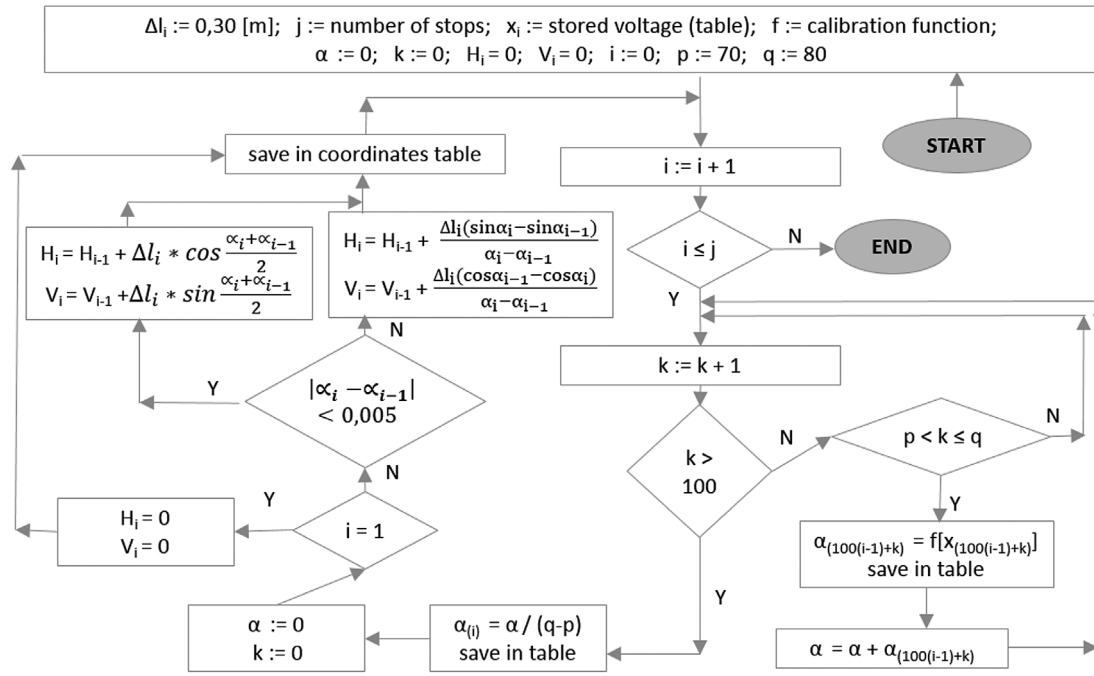


Figure 13. Algorithm of route tracking – block scheme.

Algorithm of route tracking

Knowing safe ranges of voltage value stabilisation during probe pulling, an algorithm of route tracking could have been built. Considerations were started with a general, well-known relationship, used for determination of a vertical and horizontal location of a point (probe) in a given point of curvilinear route:

$$V_i = \int_0^{l_i} \sin \alpha(l) dl \quad (10)$$

$$H_i = \int_0^{l_i} \cos \alpha(l) dl \quad (11)$$

where: V_i, H_i – vertical and horizontal locations of the centre of the probe, respectively, in a point located at a certain distance l_i from the beginning of the route (measured along the route's axis coinciding in approximation with the axis of the tendon sheath), α – inclination angle of a given segment of the route dl from horizontal. This angle is calculated based on the assumed voltage–inclination calibration function.

Infinite number of segments dl in Equations (10) and (11) was changed into a finite number of arcs or segments Δl_i . It was assumed that all were of equal length. In the interval pulling Δl_i corresponds to the distance between the markers on the rope $\Delta l_i = \Delta l = \text{const.} = .30 \text{ (m)}$. With such assumptions, simple angular relationships and relationships between the arc and the chord Δc_i are applied on the curvilinear segments of the route. It can be easily proven that in each step of the probe's passage ($i - 1, i, i + 1, i + 2, \dots$) the following relationships are true:

$$\begin{aligned} V_i &= V_{i-1} + \Delta V_i = V_{i-1} + \Delta c_i \cdot \sin \frac{\alpha_i + \alpha_{i-1}}{2} \\ &= V_{i-1} + \frac{\Delta l_i (\cos \alpha_{i-1} - \cos \alpha_i)}{\alpha_i - \alpha_{i-1}} \end{aligned} \quad (12)$$

$$\begin{aligned} H_i &= H_{i-1} + \Delta H_i = H_{i-1} + \Delta c_i \cdot \cos \frac{\alpha_i + \alpha_{i-1}}{2} \\ &= H_{i-1} + \frac{\Delta l_i (\sin \alpha_i - \sin \alpha_{i-1})}{\alpha_i - \alpha_{i-1}} \end{aligned} \quad (13)$$

For linear segments and curvilinear segments with large radii, when $|\alpha_i - \alpha_{i-1}| < .005 \text{ rad}$, then $\Delta l_i \cong \Delta c_i$, relationships (12) and (13) are simplified to:

$$V_i = V_{i-1} + \Delta V_i = V_{i-1} + \Delta l_i \cdot \sin \frac{\alpha_i + \alpha_{i-1}}{2} \quad (14)$$

$$H_i = H_{i-1} + \Delta H_i = H_{i-1} + \Delta l_i \cdot \cos \frac{\alpha_i + \alpha_{i-1}}{2} \quad (15)$$

The algorithm for calculation of the coordinates of the passed route in the interval mode is schematically presented in Figure 13. Values p and q are user-defined variables denoting voltages corresponding to the stop of the probe during a given break. The values of 70 and 80 were preliminarily assumed on the scheme, which corresponds to the 8th second of each interval.

It is also worth mentioning that for recognition of the tendon sheath's route boundary conditions can be used:

- Measurable difference between vertical coordinates of the inlet and the outlet of the sheath in the tested structure or its segment,
- Horizontal distance between the inlet and the outlet of the tested sheath, which can be controlled in-situ with e.g. laser telemeter with a built-in spirit level.

Both can be freely used to correct the coordinates determined during passage of the probe, obtained with the use of the presented algorithm. Simple linear correcting functions were used for that purpose.

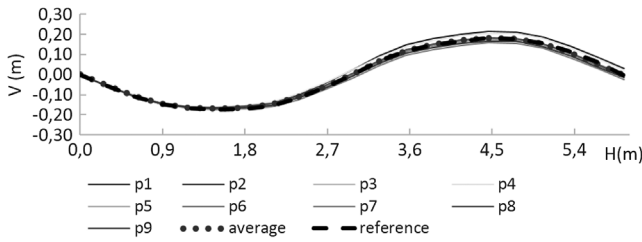


Figure 14. Route tracks obtained from the algorithm in relation to the reference route.

Results – quality of representation of the testing route

Knowing the intervals of signal stabilisation and with the use of the algorithm for route tracking, the coordinates of the probe in individual passages $p1, p2, \dots, p9$ were calculated and presented in a graphical form with broken lines depicting approximation of the route passed by the measuring probe (Figure 14).

Errors in representation of the route measured with a precise leveler (reference route) are better visible in diagrams of the deviations of coordinates determined based on the passage of the probe and measured coordinates. Figure 15(a) presents a diagram of deviations from the measured route, while Figure 15(b) displays the same relationships after consideration of boundary conditions (correction with linear functions) with respect to individual passages. Based on the collected data it can be concluded that:

- Mean deviation of the coordinates of the route obtained by averaging of the coordinates from individual passages along the route, irrespective of the way the boundary conditions were taken into consideration, was equal to 3 mm and its maximum value was equal to 9 mm,

- The maximum deviation of any vertical coordinate of a single route after consideration of boundary conditions was equal to 17 mm,
- The maximum deviation of any vertical coordinate of a single route was equal to 36 mm.

These are very promising results. The magnitude of errors in relation to a single passage correspond with allowable execution tolerances, which in a lot of cases are equal to ± 30 mm (EN 13670, 2009). Deviations of mean tracks are much lower than this value. It must be added that due to very small values of horizontal deviations they were omitted in the final conclusions.

Taking into consideration these values (and the values of deviations of the tracks from the reference route), a thesis can be formed that the discussed measurement technique, even at this stage of evolution, can be used for inventory of the layout of prestressing tendon sheaths to evaluate future global work of newly executed structures. These can be e.g. typical beam structures or box structures with curvilinear tendons in massive webs. With a higher number of passages of the probe along a given cable canal the accuracy of representation can be satisfactory to additionally evaluate local geometrical imperfections of tendons placed in thin-walled elements.

Issue of time consumption and labour intensity

Because the presented technique and the probe have been created by the authors from scratch, the development is still at the stage of laboratory tests. Nevertheless, the expected efficiency of the proposed technique in the in-situ tests is an interesting issue. To discuss this issue a simple example of a typical double-beam prestressed highway bridge can be referred (Figure 16). The bridge has two spans of 29 m each. The first potential problem

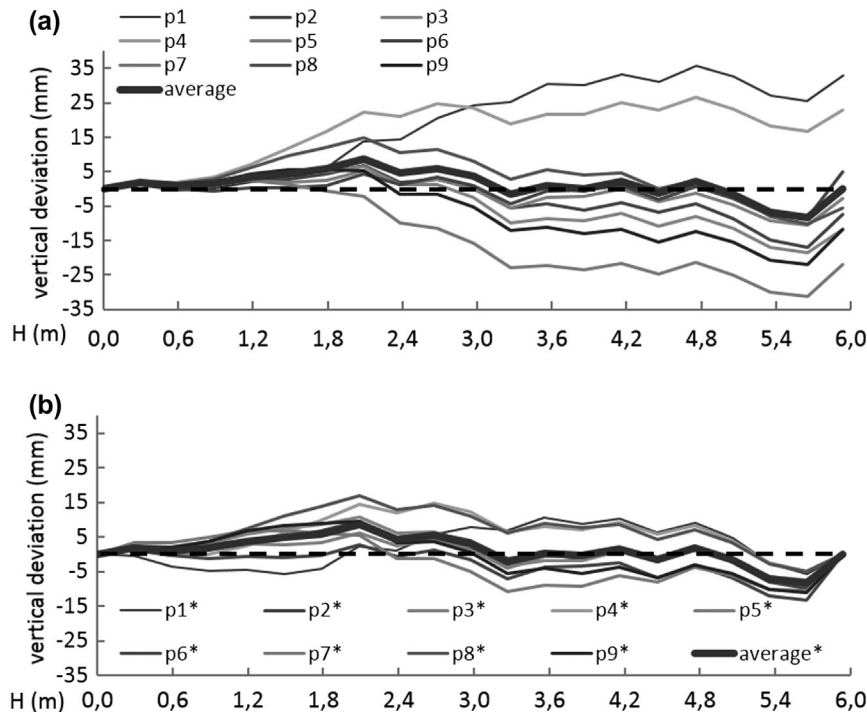


Figure 15. Deviations of coordinates calculated with the algorithm with respect to the measured coordinates (reference route). (a) deviation of coordinates. (b) deviation of coordinates with boundary conditions.

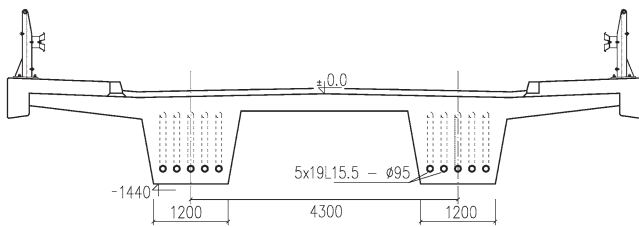


Figure 16. Cross section of typical double-beam, post-tensioned, highway bridge.

during the tests with the probe might be introduction of the pulling rope into the ~60 m long route of tendon sheath (the shape of the route complies with Figure 6). The solution is, however, simple: relatively stiff, steel ropes can be easily used and introduced manually. In case of high friction on longer routes steel rope can be replaced with a single prestressing strand and manual operations can be replaced by the use of a machine for tendon installation.

The second problem is the choice of the length of pulling interval and the number of the required passages along each sheath. It has a direct effect on time consumption and accuracy of the tests. Based on the recommendations (Topczewski, 2012) and expertise of the first author, the optimum interval length for testing of typical 19- or 22-strand tendon sheaths is equal to 30 cm. In the authors' opinion, despite a desire to reduce time consumption of the process, this value should not be increased, even at rectilinear segments because the location of geometrical imperfections is unforeseeable (Flaga & Kisała, 2013). Given the results of the performed experiment and statistical analyses it is advised that in the in-situ tests two passages are performed along each sheath (one in each direction). It has been calculated that with such a number of trials the time necessary to perform the inspection of a typical viaduct (Figure 16), with preparatory works, would take approximately 12 hours. Even if 6 passages were made, as recommended for testing of local imperfections of tendons in thin-walled structures, a probable result would be around 40 hours. In comparison, based on the experience of works (Owerko & Ortyl, 2013) the authors estimate that GPR tests on the discussed structure would take at least 50 hours. It must be emphasised that GPR is one of the most efficient and the most frequently used NDT method among the methods presented in Table 1. This comparison would further promote the testing method with MEMS accelerometer if the accessibility criterion was taken into consideration. Probing approach allows for comfortable work at the level of abutments and eliminates the need to use scaffolding or boom lifts. The proposed measurement method is independent of the degree of reinforcement or the cross-sectional shape of the girder. Low costs of the tool itself (a probe with accelerometer) in comparison to the costs of other tools used for NDT tests must be also mentioned. The authors predict that multiple probes can be simultaneously used in all sheaths, which would further decrease time consumption of the testing process.

Conclusions

Problems resulting from inaccurate assembly of prestressing tendon sheaths occur in concrete bridges of different types. The

errors are sometimes considerable and exceed by far the required tolerances of execution. They are caused by different factors and may appear both before and during casting of concrete. Some of the inaccuracies may even make proper realisation of prestressing programme impossible or lead to a catastrophe of the structure. Moreover, improper route of a tendon generates different distribution of forces than the one assumed in the design project. This is especially important in the analysis of statically indeterminate structures where accurate modelling of a prestressing system is required. The knowledge of the real layout of tendons may also appear to be valuable in expert projects which aim at determination of future serviceability of the existing structures.

Because of these needs several methods for localisation of concreted tendons have been developed. These techniques include NDT methods. For identification of prestressing tendons such methods as GPR and acoustic (UE, IE, USW) methods should be specifically mentioned. It can be concluded from an overview of the literature of the subject that their use gives often positive results. It must be, however, emphasised that a part of the published tests was performed in not too demanding conditions. The testing areas were characterised with simple geometry and reinforcement of low intensity, which does not comply with the real conditions of bridge structures. The literature of the subject emphasises also multiple resolution and efficiency limitations of the non-destructive techniques as well as high labour demand during realisation of some of the tests. The referred NDTs have also considerable accessibility requirements: it is usually necessary to build scaffoldings or use telescopic boom lifts. In case of structures which are still in formwork application of these methods is practically impossible. Regarding these issues, the main goal of this paper was to present a measurement method using a probe moving inside an empty sheath, equipped with a MEMS capacitive accelerometer. This technique is independent of the before-mentioned conditions and restrictions.

Based on the pre-determined mode of work of this equipment, the tests were performed which included nine repeatable passages of the probe along the custom-made testing route. One of its aims was to find safe intervals of the registered voltages' stabilisation. This allowed to develop an algorithm which appropriately filters a signal and at the same time allows to determine an image (track) of the route passed by the probe in the form of a broken line. Additionally, useful boundary conditions were formulated.

Finally, quality of the mapping of the testing route was assessed based on the calculated coordinates of the subsequent tracks with respect to the measured (reference) coordinates. The obtained results were satisfactory. The magnitudes of deviations correspond to the operative tolerances of execution used on numerous construction sites of bridge structures. Deviations of coordinates of the track obtained from averaging of coordinates registered during several passages were small enough to allow the presented technique not only to localise gross errors in tendons' assembly layout but also to measure local imperfections of their routes in thin-walled elements.

In the near future a series of auxiliary works are planned to improve the applied measurement system. It is planned, i.e., to slightly modify the casing to lower its centre of gravity, to equip the probe with a digital camera with LED or to extend the integrated circuit with a magnetometer. The last one would allow for

direct measurement of inclination of the sheath's route in plane. It is also considered to construct a new propelled probe with a stepmeter which would eliminate the necessity of manual pulling. Additionally, a series of tests on longer routes are planned. They will be performed in laboratory conditions or during construction of a new real structure.

Disclosure statement

No potential conflict of interest was reported by the authors.

ORCID

Piotr Owerko  <http://orcid.org/0000-0003-4698-4933>

References

- Aalami, B. O. (2000). Structural modeling of posttensioned members. *Journal of Structural Engineering*, 126, 157–162. doi:10.1061/(ASCE)0733-9445(2000)126:2(157)
- Ata, N., Mihara, S., & Ohtsu, M. (2007). Imaging of ungrouted tendon ducts in prestressed concrete by improved SIBIE. *NDT & E International*, 40, 258–264. doi:10.1016/j.ndteint.2006.10.008
- BBR. (2013). *European technical approval* (ETA – 06/0147). Retrieved from http://www.bbrnetwork.com/fileadmin/bbr_network/PDFs/Approvals/CMI/BBR-ETA-06_0147-CMI_31_EN-Rev2_0813.pdf
- Biliszczyk, J. (2013). Most MA 532 w ciągu autostrady A1 w Mszanie. Historia budowy [MA 532 bridge along the A1 motorway in Mszana. History of construction]. In J. Biliszczyk (Ed.), *Obiekty mostowe w infrastrukturze miejskiej* [Bridges in urban infrastructure] (pp. 201–219). Wrocław: Lower Silesia Educational Publishers.
- Chae, M. J., Yoo, H. S., Kim, J. Y., & Cho, M. Y. (2012). Development of a wireless sensor network system for suspension bridge health monitoring. *Automation in Construction*, 21, 237–252. doi:10.1016/j.autcon.2011.06.008
- Cheilakou, E., Theodorakas, P., Kouli, M., Moustakidis, S., & Zeris, C. (2013). *Determination of reinforcement and tendon ducts positions on pre-stressed concrete bridges by means of ground penetrating radar (GPR)*. Presented at the 5th international conference on NDT of HSNT – IC MINDT, Athens Greece. doi:10.1117/12.2046354
- Choi, C.-K., Kim, K.-H., & Hong, H.-S. (2002). Spline finite strip analysis of prestressed concrete box-girder bridges. *Engineering Structures*, 24, 1575–1586. doi:10.1016/S0141-0296(02)00101-3
- Cruz, P. J. S., Topczewski, L., Fernandes, F. M., Trela, C., & Lourenço, P. B. (2010). Application of radar techniques to the verification of design plans and the detection of defects in concrete bridges. *Structure and Infrastructure Engineering*, 6, 395–407. doi:10.1080/15732470701778506
- Daniels, D. J. (2004). *Ground penetrating radar*. London: Institution of Engineering and Technology.
- De La Haza, A. O., Samokrutov, A. A., & Samokrutov, P. A. (2013). Assessment of concrete structures using the Mira and Eyecon ultrasonic shear wave devices and the SAFT-C image reconstruction technique. *Construction and Building Materials*, 38, 1276–1291. doi:10.1016/j.conbuildmat.2011.06.002
- Dérobot, X., Aubagnac, C., & Abraham, O. (2002). Comparison of NDT techniques on a post-tensioned beam before its autopsy. *NDT & E International*, 35, 541–548. doi:10.1016/S0963-8695(02)00027-0
- Dywidag. (2013). *European technical approval* (ETA – 06/0025). Retrieved from <http://www.dywidag-norge.no/wp-content/uploads/2013/09/DSI-SUSPA-ETA-06-0025-SUSPA-Strand.pdf>
- EN 13670. (2009). Execution of concrete structures. European Standard. European Committee for Standardization. ICS 91.080.40 - Concrete structures. Retrieved from https://standards.cen.eu/dyn/www/f?p=204:110:0:::FSP_PROJECT,FSP_ORG_ID:32601,6087&cs=1242D2BAC809BE1E652D0601808A56B23
- Flaga, K., & Kisała, D. (2013). Wpływ imperfekcji geometrycznych kabli sprężających na dodatkowe wyężenie płyty dolnej dźwigarów mostowych o przekroju skrzynkowym [The influence of geometric imperfections of prestressing tendons on the additional load of the box girder bottom plate]. *Inżynieria i Budownictwo* [Engineering and construction], 69, 631–637.
- Freyssinet. (2010). *European technical approval* (ETA – 10/0326). Retrieved from <http://www.freyssinet.es/wp/wp/wp-content/uploads/2013/03/ETA100326acopladorfreyssinet.pdf>
- Geokon Incorporated. (2015). The 6000 and 6100 series portable inclinometer probes. Retrieved from http://www.geokon.com/content/datasheets/6000_6100_Series_Inclinometer_Probes.pdf
- Gocał, J., Ortyl, Ł., Owerko, T., Kuras, P., Kocierz, R., Ćwiakła, P., ... Bałut, A. (2013). *Determination of displacements and vibrations of engineering structures using ground-based radar interferometry*. Kraków: AGH University. Retrieved from <http://winntbg.bg.agh.edu.pl/skrypt4/0552/determination.pdf>
- International Atomic Energy Agency. (2002). *Guidebook on non-destructive testing of concrete structures*. Retrieved from http://www-pub.iaea.org/mtcd/publications/pdf/tcs-17_web.pdf
- Kavitha, S., Joseph Daniel, R., & Sumangala, K. (2016). High performance MEMS accelerometers for concrete SHM applications and comparison with COTS accelerometers. *Mechanical Systems and Signal Processing*, 66–67, 410–424. doi:10.1016/j.ymssp.2015.06.005
- Kohl, C., & Streicher, D. (2006). Results of reconstructed and fused NDT-data measured in the laboratory and on-site at bridges. *Cement and Concrete Composites*, 28, 402–413. doi:10.1016/j.cemconcomp.2006.02.005
- Landuyt, D. W. V. (1991). *The effect of duct arrangement on breakout of internal post-tensioning tendons in horizontally curved concrete box girder webs*. University of Texas at Austin. Retrieved from <https://fsl.engr.utexas.edu/pdfs/Van%20Landuyt,%20Dean%20William.pdf>
- Łaziński, P., & Salamak, M. (2011). Identification of computational models in load carrying structures of concrete bridges on the basis of making load tests. In *Proceedings of the 7th Central European Congress on concrete engineering CCC 2011* (pp. 353–356). Balatonfüred. Retrieved from https://www.researchgate.net/profile/Marek_Salamak/publication/256472414_Identification_of_computational_models_in_load_carrying_structures_of_concrete_bridges_on_the_basis_of_making_load_tests/links/004635239fa191526d000000.pdf
- Łaziński, P., & Salamak, M. (2015). Load test of extremely wide extradosed concrete bridge. In *Proceedings of the 11th Central European Congress on concrete engineering CCC 2015* (pp. 302–305). Hainburg. Retrieved from https://www.academia.edu/16622251/Load_test_of_extremely_wide_extradosed_concrete_bridge
- Martin, J., Broughton, K. J., Giannopolous, A., Hardy, M. S. A., & Forde, M. C. (2001). Ultrasonic tomography of grouted duct post-tensioned reinforced concrete bridge beams. *NDT & E International*, 34, 107–113. doi:10.1016/S0963-8695(00)00035-9
- Muldoon, R., Chalker, A., Forde, M. C., Ohtsu, M., & Kunisue, F. (2007). Identifying voids in plastic ducts in post-tensioning prestressed concrete members by resonant frequency of impact-echo, SIBIE and tomography. *Construction and Building Materials*, 21, 527–537. doi:10.1016/j.conbuildmat.2006.04.009
- Mutsuyoshi, H., Hai, N. D., & Kasuga, A. (2008). *Recent technology of prestressed concrete bridges in Japan*. Presented at the 3rd ACF international conference – ACF/VCA, Ho Chi Minh. Retrieved from <http://www.iabse-bd.org/old/43.pdf>
- Owerko, P., & Ortyl, Ł. (2013). GPR identification of prestressing tendons in areas with high density of ordinary reinforcement. *13th International Multidisciplinary Scientific GeoConferences, Science and Technologies in Geology, Exploration and Mining*, 2, 771–778. doi:10.5593/SGEM2013/BA1.V2/S05.012
- Owerko, P., Ortyl, Ł., & Salamak, M. (2013). *Identification of prestressing tendons using ground penetrating radar in particular the anchorage zone*. Presented at the 9th Central European Congress on concrete engineering CCC 2013, Concrete Structures in Urban Areas, Wrocław.
- Papoulis, A., & Pillai, S. U. (2002). *Probability, random variables and stochastic processes* (4th ed.). London: McGraw-Hill.

- Podolny, W. (1985). The cause of cracking in post-tensioned concrete box girder bridges and retrofit procedures. *Journal of the Prestressed Concrete Institute*, 30, 82–139.
- Ruan, X., Shi, X., & Li, X. (2012). Failure analysis of tendon breakout on bottom slab of a pre-stressed concrete box gird bridge during construction. *Engineering Failure Analysis*, 25, 291–303. doi:10.1016/j.engfailanal.2012.05.017
- Silvestri, C., & Williams, W. (2012). *Rebar locator for pinned precast barrier application* (No. 405160-32). TX: Roadside Safety Research Program. Retrieved from http://www.roadsidepooledfund.org/files/2012/08/405160-32_Final-2012-08-31.pdf
- Topczewski, L. (2007). *Improvement and application of ground penetrating radar non-destructive technique for the concrete bridge inspection* (doctoral dissertation). University of Minho, Guimarães. Retrieved from <http://repositorium.sdum.uminho.pt/handle/1822/6755>
- Topczewski, L. (2012). Guidelines for the application of ground penetrating radar (GPR) to inspection of concrete bridges – Reflection mode. *Roads and Bridges – Drogi i Mosty*, 11, 329–343. doi:10.7409/rabdim.012.005
- U.S. Federal Highway Administration. (2013). *Post-tensioning tendon installation and grouting manual*. Retrieved from <https://www.fhwa.dot.gov/bridge/construction/pubs/hif13026.pdf>
- Verma, S. K., Bhadauria, S. S., Akhtar, S., Verma, S. K., Bhadauria, S. S., & Akhtar, S. (2013). Review of nondestructive testing methods for condition monitoring of concrete structures. *Journal of Construction Engineering*, 2013, 1–12. doi:10.1155/2013/834572
- Xie, X., Qin, H., Yu, C., & Liu, L. (2013). An automatic recognition algorithm for GPR images of RC structure voids. *Journal of Applied Geophysics*, 99, 125–134. doi:10.1016/j.jappgeo.2013.02.016
- Yehia, S., Qaddoumi, N., Farrag, S., & Hamzeh, L. (2014). Investigation of concrete mix variations and environmental conditions on defect detection ability using GPR. *NDT & E International*, 65, 35–46. doi:10.1016/j.ndteint.2014.03.006
- Zhou, X. Y., Luan, J., & Zhang, D. H. (2013). Inspection of grouting quality for grouted tendon ducts using ground penetrating radar technique. *Advanced Materials Research*, 639–640, 1051–1055. doi:10.4028/www.scientific.net/AMR.639-640.1051
- Zilch, K., Weiher, H., & Riesemann, M. (2007). *Concrete bridges in Germany*. Retrieved from https://www.researchgate.net/profile/Hermann_Weiher/publication/242116830_Concrete_Bridges_in_Germany/links/0deec532160cda0b46000000.pdf